HOKKAIDO UNIVERSITY

Title	The intercellular expression of type-XVII collagen, laminin-332, and integrin-beta 1 promote contact following during the collective invasion of a cancer cell population
Author(s)	Kumagai, Yuji; Nio-Kobayashi, Junko; Ishida-Ishihara, Sumire; Tachibana, Hiromi; Omori, Ryosuke; Enomoto, Atsushi; Ishihara, Seiichiro; Haga, Hisashi
Citation	Biochemical and biophysical research communications, 514(4), 1115-1121 https://doi.org/10.1016/j.bbrc.2019.05.058
Issue Date	2019-07-05
Doc URL	http://hdl.handle.net/2115/78009
Rights	© 2019 This manuscript version is made available under the CC-BY-NC-ND 4.0 license http://creativecommons.org/licenses/by-nc-nd/4.0/
Rights(URL)	http://creativecommons.org/licenses/by-nc-nd/4.0/
Type	article (author version)
File Information	BBRC-S-19-07139-1.pdf

Instructions for use

Hokkaido University Collection of Scholarly and Academic Papers : HUSCAP

Elsevier Editorial System(tm) for
Biochemical and Biophysical Research Communications
Manuscript Draft

Manuscript Number:

Title: The intercellular expression of type-XVII collagen, laminin-332, and integrin-β1 promote contact following during the collective invasion of a cancer cell population

Article Type: Short communication/Full length article

Keywords: Collective invasion
Contact following
Integrin-β1
Laminin-332
Type-XVII collagen

Corresponding Author: Professor Hisashi Haga,

Corresponding Author's Institution: Hokkaido University

First Author: Yuji Kumagai

Order of Authors: Yuji Kumagai; Junko Nio-Kobayashi; Sumire Ishida-Ishihara; Hiromi Tachibana; Ryosuke Omori; Atsushi Enomoto; Seiichiro Ishihara; Hisashi Haga

Highlights

Integrin-β1 is localized to the intercellular site in a cancer cell population.

Integrin-β1 activity promotes contact following in collective invasion.

ECM proteins are localized to the intercellular site in a cancer cell population.

Expressions of ECM proteins are required for contact following in collective invasion.

Title page

The intercellular expression of type-XVII collagen, laminin-332, and integrin-β1 promote contact following during the collective invasion of a cancer cell population

Yuji Kumagai[a], Junko Nio-Kobayashi[b], Sumire Ishida-Ishihara[c], Hiromi Tachibana[a], Ryosuke Omori[d], Atsushi Enomoto[e], Seiichiro Ishihara[c, f], Hisashi Haga[c, f, *]

[a]Division of Life Science, Graduate School of Life Science, Hokkaido University, N10-W8, Kita-ku, Sapporo 060-0810, Japan

[b]Laboratory of Histology and Cytology, Faculty of Medicine and Graduate School of Medicine, Hokkaido University, N15-W7, Kita-ku Sapporo, 060-8638, Japan

[c]Department of Advanced Transdisciplinary Sciences, Faculty of Advanced Life Science, Hokkaido University, N10-W8, Kita-ku, Sapporo 060-0810, Japan

[d]Division of Bioinformatics, Research Center for Zoonosis Control, Hokkaido University, N20-W10, Kita-ku, Sapporo 001-0020, Japan

[e]Department of Pathology, Graduate School of Medicine, Nagoya University, 65 Tsurumai-cho, Showa-ku, Nagoya 466-8550, Japan

[f]Soft Matter GI-CoRE, Hokkaido University, N21-W11, Kita-ku, Sapporo 001-0021, Japan

*To whom correspondence should be addressed: Hisashi Haga

E-mail address: haga@sci.hokudai.ac.jp

Fax: +81 11 706 4909.

Abstract

Cancer cells can invade as a population in various cancer tissues. This phenomenon is called collective invasion, which is associated with the metastatic potential and prognosis of cancer patients. The collectiveness of cancer cells is necessary for collective invasion. However, the mechanism underlying the generation of collectiveness by cancer cells is not well known. In this study, the phenomenon of contact following, where neighboring cells move in the same direction via intercellular adhesion, was investigated. An experimental system was created to observe the two-dimensional invasion using a collagen gel overlay to study contact following in collective invasion. The role of integrin-β1, one of the major extracellular matrix (ECM) receptors, in contact following was examined through the experimental system. Integrin-β1 was localized to the intercellular site in squamous carcinoma cells. Moreover, the intercellular adhesion and contact following were suppressed by treatment of an integrin-β1 inhibitory antibody. ECM proteins such as laminin-332 and type-XVII collagen were also localized to the intercellular site and critical for contact following. Collectively, it was demonstrated that the activity of integrin-β1 and expression of ECM proteins in the intercellular site promote contact following in the collective invasion of a cancer cell population.

Keywords

Collective invasion

Contact following

Integrin-β1

Laminin-332

Type-XVII collagen

1. Introduction

Most cancer-related deaths are caused by metastasis; secondary tumors are formed in the organs away from the primary tumor. In the early stages of metastasis, cancer cells spread into normal peripheral tissues [1]. This phenomenon is called an invasion, which significantly affects the prognosis of cancer patients [2]. Cancer cells have a variety of invasive patterns [3]. Many previous studies have focused on “individual invasion” such as amoeboid and mesenchymal invasion [4]. On the other hand, collective invasion, in which cancer cells invade as a cell population maintaining the epithelial morphology, has only recently come to light [5]. Collective invasion has been observed in various cancer tissues and is associated with cancer metastasis [6]. Therefore, it is considered that collective invasion is a critical phenomenon of invasive cancer cells. However, the molecular mechanism of collective invasion is not currently well understood.

Integrins are transmembrane proteins that function as extracellular matrix (ECM) receptors [7]. Integrin-β1, a receptor for collagen, laminin, and fibronectin, linked to actin filament (F-actin). Thus, integrin-β1 plays a crucial role in cell motility and cell division by mediating the linkage of the ECM and the cytoskeleton [8]. Furthermore, integrin-β1 is required for collective invasion in cutaneous squamous carcinoma cells (SCC) [9]. In this way, integrin-β1 contributes to cancer progression by promoting cancer cell invasion. However, the molecular mechanisms behind this invasion, including how integrin-β1 promotes collective invasion, are not currently well known.

Collectiveness in cancer cells is necessary for collective invasion. This study focuses on contact following, the phenomenon which provides intercellular adhesion for the movement of neighboring cells in the same direction, to investigate the mechanism in cancer cells which induces collectiveness. Contact following was proposed to account for the collective migration of Dictyostelium [10]. In addition, contact following also occurs in the collective migration of MDCK epithelial cells [11]. As shown in our previous studies, integrin-β1 is necessary for the collectiveness of MDCK cells [12]. Therefore, we hypothesize that integrin-β1 promotes collective behaviors by contributing to contact following.

In this study, we demonstrated that integrin-β1 is localized to the intercellular sites in a cancer cell population and its activity is essential to contact following. Furthermore, the expression of ECM proteins in the intercellular site is also required for contact following. The findings in this study suggest the interaction between integrin-β1 and ECM proteins promotes collective invasion via the regulation of contact following.

2. Materials and Methods

2.1. Cell culture

A431 cells were obtained from the American Type Culture Collection and were cultured in Dulbecco's Modified Eagle Medium (Sigma-Aldrich Co. LLC, St Louis, MO, USA) supplemented with 10% fetal bovine serum (Sigma-Aldrich Co. LLC) and 1% antibiotic/antimycotic solution (Sigma-Aldrich Co. LLC). The cells were cultured in a humidified incubator at 37°C and 5% CO2.

2.2. Collagen gel overlay conditions

We used type-I collagen (1.6 mg/mL, Cell matrix I-P, Nitta Gelatin, Osaka, Japan) for collagen gel overlay conditions. A 24-well cell culture plate was filled with 200 μL of collagen solution and incubated at 37°C for 30 min to induce gelation. The collagen solution was poured onto the cells 24 hours after cell seeding ($8x10^4$) on the collagen gel, and incubated for 30 min at 37°C to induce gelation. All experiments in this study were carried out using this experimental system.

2.3. Construction of plasmids and developing cell lines

To construct the Emerald-Histone H2B encoding vector, Histone H2B encoding DNA was amplified by PCR using pKanCMV-mClover3-10aa-H2B (Addgene, Cambridge, MA, USA) and KOD-Plus (TOYOBO, Osaka, Japan). The primer set used for PCR is as follows: 5’-AAAGGATCCGCCACCATGCCTGAACCGGCAAAATC-3’ (forward) and 5’-

AAAGAATTCAACTTGGAGCTGGTGTACTTGGTGAC-3’ (reverse). The fusion protein of Histone H2B and Emerald, a green fluorescent protein, was inserted into MCS of pIRES-ZsGreen 1 Vector (Clontech Laboratories, lnc., Palo Alto, California, USA). Puromycin-resistant genes were inserted in exchange with ZsGreen and linked to Emerald-Histone H2B using IRES linker. Selective cultures were performed using a culture media containing 2 μg/mL puromycin after transfection into A431-WT using Viafect transfection reagent (Promega, Madison, WI, USA).

2.4. Time-lapse observation

Time-lapse observations in the bright field and the fluorescent field were performed using a phase-contrast microscope (TE2000, Nikon, Tokyo, Japan) equipped with a 20X objective lens. NIS-Elements Advanced Research software (Nikon) was used to capture images for time-lapse observation. The Images in the bright field were captured every 5 min for 16 hours and the images in the fluorescent field were captured every 20 min for 16 hours. A stage top incubator (STG-WSKMX-SET, Tokai Hit Co., Shizuoka, Japan) was used to maintain the samples at 37°C.

2.5. Immunofluorescent staining

Cells cultured in collagen gel overlay conditions were fixed with 4% paraformaldehyde (Nacalai tesque, Kyoto, Japan) for 1 hour at 4°C and permeabilized with 0.1% saponin (Wako Pure Chemical Industries, Osaka, Japan) for 10 minutes at 25°C. Blocking was performed using

1% bovine serum albumin (BSA, Wako Pure Chemical Industries) in phosphate buffer saline for 1 hour at 37°C. Cells were incubated with a primary antibody diluted in Can Get Signal immunostain (Immunoreaction Enhancer Solution B, TOYOBO) overnight at 4°C. Anti-integrin-β1 (1:200, AIIB2, Developmental Studies Hybridoma Bank at the University of Iowa, Iowa City, IA), anti-COL17 (1:500, EPR18614, Abcam Plc., Cambridge, UK), anti-laminin-α3 (1:100, P3H9, Developmental Studies Hybridoma Bank at the University of Iowa), anti-laminin-β3 (1:500, 610423, BD Biosciences, San Jose, CA, USA), and anti-phosphorylated Tyr397 FAK (1:500, EP2160Y, Abcam Plc.) were used as primary antibodies. Next, the cells were incubated with a secondary antibody diluted with Can Get Signal immunostain (Immunoreaction Enhancer Solution B, TOYOBO) and Alexa Fluor-546 phalloidin (1:500, Invitrogen, Carlsbad, CA) for 1 hour at 25°C. Alexa Fluor-488 anti-mouse IgG (1:500, Invitrogen) and Alexa Fluor-488 anti-rabbit IgG (1:500, Invitrogen) were used as secondary antibodies. Fluorescent images were captured by confocal laser microscopy (A1R Confocal Imaging System, Nikon).

2.6. Immunoelectron microscopy

A431 cells were processed for the pre-embedding silver-intensified immunogold method as described in a previous study [13]. AIIB2 (1:200) was used as the primary antibody. Nanogold-anti rat IgG (1:100, Nanoprobes, Yaphank, NY, USA) was used as the secondary antibody. Signals from the gold were enhanced using HQ silver (Nanoprobes). Observations were carried out using a transmission electron microscope (H7100, Hitachi High-Technologies

Corp., Tokyo, Japan).

2.7. Inhibitor treatment

A431 cells in collagen gel overlay conditions were treated with AIIB2 or normal rat IgG (Wako Pure Chemical Industries). Each antibody was used at 2 μg/mL. Time-lapse observations were performed immediately after treatment with inhibitors.

2.8. Cell tracking

Cell nuclei were automatically tracked using the TrackMate plug-in from Image J software to track cell movement (National Institutes of Health, Bethesda, MD) [14].

2.9. Quantification of contact following

Contact following was evaluated using cosine function. Cosine values were calculated from the angle between the movement directions of neighboring cells over 20 min. Cells within 100 μm of a targeted cell were analyzed. The analysis was performed on all cells of the population.

2.10. Small interfering RNA (siRNA) transfection

Cells were transfected with the appropriate siRNA or random RNA with Lipofectamine RNAiMAX Reagent (Thermo Fisher Scientific, Inc. Waltham, MA, USA). The following target sequences were used: COL17A1: 5'- TGGATGTAACCAAGAAAAACAAA-3' (sense sequence), LAMA3: 5'- CAGTGATAAACTGTTAAATGAAG-3' (sense sequence), LAMB3:

5’- CACAAACTTGAGAGTCAATTTCA-3’ (sense sequence), and negative control: 5’-TTCAACTGTGATAGATCCAAT-3’ (sense sequence).

2.11. Immunoprecipitation

Cells were solubilized in lysis buffer. The cell lysates were incubated with anti-COL17 (EPR18614, Abcam Plc.) or normal rabbit IgG (Wako Pure Chemical Industries) for 24 hours at 4°C. Each antibody was used at 15 μg/mL. The immune complexes were obtained using Capturem IP & Co-IP Kit (Takara-Bio Inc., Shiga, Japan) and analyzed by Western blotting.

2.12. Western blotting

Western blotting was performed as previously reported [15]. Anti-integrin-β1 (1:2,000, 610467, BD Biosciences), anti-laminin-β3 (1:1,000, 610423, BD Biosciences), anti-COL17 (1:1,000, EPR18614, Abcam Plc.), and anti-glyceraldehyde 3-phosphate dehydrogenase (1:1,000,000, AM4300, Thermo Fisher Scientific, Inc.) were used as primary antibodies. Horseradish peroxidase (HRP) conjugated anti-mouse IgG (1:10,000, Cell Signaling Technology, Inc., Danvers, MA, USA) and HRP conjugated anti-rabbit IgG (1:10,000, Cell Signaling Technology, Inc.) were used as secondary antibodies. Protein signals were detected with Immobilon Western Chemiluminescent HRP substrate (EMD Millipore, Billerica, MA, USA).

2.13. Quantitative PCR

RNA extraction, reverse transcription reaction, and quantitative PCR were performed as

previously reported [16]. The primer sequences used were; LAMA3: 5’-TGGGATGGCTGTGGATCTTTGG-3’ (forward), 5’-CACCCTTTGCTGCTGTGAACTG-3’ (reverse).

2.14. Statistical analysis

Each experiment was independently repeated at least three times. P-values less than 0.05 were considered statistically significant. Contact following was described as cosine value and graphed by box-plot using the R software ver. 3.3.3 (R Development Core Team, Vienna, Austria) (Fig. 2F and 3E). Comparisons of contact following were performed via the Wilcoxon rank sum test with Bonferroni correction (Fig. 2F and 3E). The signal intensity in western blotting was graphed using Microsoft Excel (Microsoft corp., Redmond, USA) (Fig. 4D). Comparisons of this signal intensity were performed using Welch’s t-test after testing the normality of these datasets (Shapiro-Wilk test, $P > 0.95$; Fig. 4D). All tests in this study were performed using the R software ver. 3.3.3.

3. Results

3.1. Collective invasion of A431 cells in collagen overlay culture conditions

Cell movement was tracked by observing collective invasion to analyze the contact following of cancer cells. In the existing experimental system for collective invasion, cancer cells move in a three-dimensional direction [17]. However, to track cell movement directly, it is desirable for cells to move in a two-dimensional direction. Therefore, we established a new experimental system for collective invasion to observe cell movement in the two-dimensional direction. Collagen gel overlay conditions were used as an experimental system, and A431 cutaneous squamous carcinoma cells (SCCs) with collective invasive potential were cultured (Fig. 1A). The two-dimensional collective movement of A431 cells in collagen gel overlay conditions was observed as a result of time-lapse observation in the bright field (Fig. 1B and Movie 1). In addition, the cell line expressing the nuclear localized fluorescent protein (A431-H2B) was established to track cell movement. A431-H2B also showed two-dimensional collective movement (Fig. S1A and Movie 2), and cell movement was successfully automatically tracked. Therefore, this experimental system was used as a model of collective invasion.

3.2. Integrin-β1 is localized to the intercellular site and required for intercellular adhesion and contact following

This study found that the high expression of integrin-β1 in the leading cells contributes to the collective behaviors of MDCK cells and SCC [9, 12]. Therefore, the localization of integrin-β1 in collagen overlay conditions with immunofluorescent staining was first investigated. It was found that integrin-β1 is uniformly localized to the intercellular site as a result of immunofluorescent staining (Fig. 2A). In addition, immunofluorescent staining with anti-active integrin-β1 antibodies revealed that intercellular integrin-β1 is its active form (Fig. S1B). Next, immunoelectron microscopy was carried out to investigate the structure of the intercellular adhesion and localization of integrin-β1 in detail. As a result, A431 cells were found to have an adherens junction at the intercellular site, while integrin-β1, and not the adherens junction, was localized to the cell surface (Fig. 2B). Subsequently, A431 cells were treated with AIIB2, which is an inhibitory antibody of active integrin-β1, and time-lapse observations, as well as treatments, were undertaken in the bright field. As a result, the inhibition of active integrin-β1 by AIIB2 suppressed the intercellular adhesion in A431 cells (Fig. 2C and Movie 3, 4). These results suggest that integrin-β1 plays a role in the intercellular site which is essential for intercellular adhesion.

The role of integrin-β1 in contact following of a collective invasion was investigated. First, a method was developed to analyze contact following (Fig. 2D). When cell A was the target, the analysis was performed on the cells within a 100-μm radius of cell A. Keeping this in mind and using the example described in Fig. 2D, cell B qualifies as the analysis target of cell A, while cell C does not. Finally, the cosine of the angles between the movement directions of cells A and B after 20 min was calculated to measure the strength of contact following between the two

cells. In this way, a cosine approaches 1 when contact following is strong and approaches -1 when contact following is weak. This analysis was performed on all cells of the cell population. The influence of AIIB2 on contact following with A431-H2B is shown in Fig. 2E and Movies 5 and 6. As a result of the quantitative analysis, AIIB2 significantly suppressed contact following (Fig. 2F). From this result, it was found that the activity of the intercellular integrin-β1 is required for contact following.

3.3. ECM proteins are localized to the intercellular site and are required for contact following

As previously described, integrin-β1 is a representative ECM receptor [7]. In addition, the activity of intercellular integrin-β1 is required for intercellular adhesion and contact following. Therefore, we hypothesize that ECM proteins are localized to the intercellular site. By investigating the localization of several ECM proteins with immunofluorescent staining, it was found that type-XVII collagen (COL17) is localized to the intercellular sites (Fig. 3A). COL17 is a transmembrane collagen, but its extracellular domain is secreted into the surrounding ECM as its cleavage form [18]. It was confirmed that the cleavage form of COL17 is secreted in A431 cells (Fig. S1C). In addition, laminin-α3 and laminin-β3 constituting of laminin-332 are also localized to the intercellular sites (Fig. 3B, C).

Next, the gene expression of intercellular ECM proteins was depleted with small interference RNA (siRNA) (Fig. S1D-F) to investigate the role of intercellular ECM proteins. Depletion of ECM protein expression significantly suppressed contact following (Fig. 3D, E and Movie

7-10). Therefore, it was found that the expression of intercellular ECM proteins is also required for contact following. Furthermore, these results suggest that the interaction between integrin-β1 and ECM proteins in the intercellular sites promotes contact following in collective invasion.

3.4. The interaction between integrin-β1 and ECM proteins

The interactions between integrin-β1, COL17, and laminin-332 were then investigated. Previous studies suggest that there is binding between integrin-β1 and COL17 [19]. Therefore, whether integrin-β1 and COL17 form a complex by immunoprecipitation (IP) using anti-COL17 antibody and western blotting was investigated. As a result of the IP experiment, integrin-β1 was not detected in the obtained IP fraction of COL17 (Fig. 4A). Thus, it has not been possible to prove a complex formation of integrin-β1 and COL17. Next, the complex formation between COL17 and laminin-332 was investigated. As a result of the IP experiment, laminin-β3 was detected in the obtained IP fraction of COL17 (Fig. 4B). As laminin-332 is the major ligand of integrin-β1 [20], it was hypothesized that COL17 affects interactions between integrin-β1 and laminin-332. Therefore, the influence of COL17 depletion on laminin-332 expression was investigated (Fig. 4C). As a result of quantification, COL17 depletion significantly suppressed laminin-β3 levels (Fig. 4D). Therefore, it is suggested that the COL17 level modulates the interaction between integrin-β1 and laminin-332 by controlling laminin-332 levels.

Focal adhesion kinase (FAK) is a major downstream molecule of integrin-β1 [21]. Immunofluorescent staining revealed that phosphorylated FAK (Tyr397) is localized to the intercellular site (Fig. S2A). The influence of AIIB2 on the phosphorylation of FAK was then assessed. Although intercellular adhesion was suppressed by AIIB2 treatment, phosphorylation of FAK was not inhibited (Fig. S2B). Therefore, it is believed that there are other downstream molecules of integrin-β1 in the contact following of A431 cells.

4. Discussion

In this study, we established a new experimental system for the analysis of contact following in collective invasion. A431 cells showed two-dimensional collective movement in collagen gel overlay conditions. In addition, this system enabled the automatic tracking of cell movement, whereby contact following in collective invasion could be investigated. Moreover, cancer cells needed several days to invade in the existing experimental system for collective invasion [17]. However, A431 cells invaded on a short time scale of a few hours in our experimental system. As a result, experimental tools acting immediately such as molecular inhibitors and siRNA could be used. Furthermore, a new method was also developed to analyze contact following using the cosine function. When movement direction is measured using an angle, the measurement becomes a circular variable that ranges from 0 to 360 degrees. Therefore, in contact following analysis, x and (360-x) degrees refer to the same direction. However, cosine functions determine the association of directions uniquely i.e., $\cos(x) = \cos(360-x)$. Thus, cosine transformation does not require the circular statistics method to analyze contact following.

The activity of integrin-β1 in the intercellular site was found to regulate contact following in collective invasion. Moreover, this study shows that laminin-332, a ligand of integrin-β1, is localized to the intercellular site and is required for contact following. Furthermore, COL17 levels modulate contact following via the regulation of laminin-332 levels.

Integrin-β1 contributes to not only cell-matrix adhesion but also intercellular adhesion. [22]. In addition, structural ECM mediates intercellular adhesion by integrin-β1 in glioblastoma [23].

In A431 cells, laminin-332 is localized to the intercellular site and is required for collectiveness. Laminin-332 is a major component of the basement membrane [24]. Therefore, it was considered that the basement membrane-like structural ECM consisting of laminin-332 exists in the intercellular site in A431 cells. However, it was not possible to observe a structural ECM in the intercellular site through electron microscopy. Laminin-332 promotes cancer progression as not only structural ECM but also autocrine soluble factor via binding to cell surface integrins [25]. Therefore laminin-332 is expected to act as a soluble factor in the collective invasion of A431 cells.

COL17 is cleaved by protease on the cell surface, whereby the extracellular domain is secreted into the surrounding ECM [18]. The extracellular cleavage of COL17 is essential for correct cutaneous basement membrane formation by contributing to the stabilization of laminin-332 [26]. In this study, it is shown that the cleavage form of COL17 is secreted in A431 cells and COL17 levels control laminin-β3 levels, which is a constituent of laminin-332. Therefore, it is suggested that COL17 levels modulate the interaction between integrin-β1 and laminin-332 by regulating LAMB3 levels, whereby COL17 contributes to contact following.

From the results in this study, we suggest that this interaction is a key regulator of contact following in cancer cell collective invasion. Therefore, inhibition of this interaction may be an effective way to suppress collective invasion in cancer cells.

Acknowledgments

This work was supported by JSPS KAKENHI grant numbers 17K07150 to H.H.; Advanced Research and Development Programs for Medical Innovation by Japan Agency for Medical Research and Development to H.H. and A.E; Global station for Soft Matter, a project of Global Institution for Collaborative Research and Education at Hokkaido University to H.H. and S.I.

[1] I.J. Fidler, Tumor heterogeneity and the biology of cancer invasion and metastasis, Cancer Res 38 (1978) 2651-2660.

[2] A. Breslow, Thickness, cross-sectional areas and depth of invasion in the prognosis of cutaneous melanoma, Ann Surg 172 (1970) 902-908.

[3] P. Friedl, J. Locker, E. Sahai, J.E. Segall, Classifying collective cancer cell invasion, Nat Cell Biol 14 (2012) 777-783. 10.1038/ncb2548.

[4] M. Yilmaz, G. Christofori, EMT, the cytoskeleton, and cancer cell invasion, Cancer Metastasis Rev 28 (2009) 15-33. 10.1007/s10555-008-9169-0.

[5] C. Gaggioli, S. Hooper, C. Hidalgo-Carcedo, R. Grosse, J.F. Marshall, K. Harrington, E. Sahai, Fibroblast-led collective invasion of carcinoma cells with differing roles for RhoGTPases in leading and following cells, Nat Cell Biol 9 (2007) 1392-1400. 10.1038/ncb1658.

[6] A.A. Khalil, O. Ilina, P.G. Gritsenko, P. Bult, P.N. Span, P. Friedl, Collective invasion in ductal and lobular breast cancer associates with distant metastasis, Clin Exp Metastasis 34 (2017) 421-429. 10.1007/s10585-017-9858-6.

[7] R.O. Hynes, Integrins: bidirectional, allosteric signaling machines, Cell 110 (2002) 673-687.

[8] S.P. Palecek, J.C. Loftus, M.H. Ginsberg, D.A. Lauffenburger, A.F. Horwitz, Integrin-ligand binding properties govern cell migration speed through cell-substratum adhesiveness, Nature 385 (1997) 537-540. 10.1038/385537a0.

[9] T. Kato, A. Enomoto, T. Watanabe, H. Haga, S. Ishida, Y. Kondo, K. Furukawa, T. Urano, S. Mii, L. Weng, M. Ishida-Takagishi, M. Asai, N. Asai, K. Kaibuchi, Y. Murakumo, M. Takahashi, TRIM27/MRTF-B-dependent integrin beta1 expression defines leading cells in cancer cell

collectives, Cell Rep 7 (2014) 1156-1167. 10.1016/j.celrep.2014.03.068.

[10] T. Umeda, K. Inouye, Possible role of contact following in the generation of coherent motion of Dictyostelium cells, J Theor Biol 219 (2002) 301-308.

[11] D. Li, Y.L. Wang, Coordination of cell migration mediated by site-dependent cell-cell contact, Proc Natl Acad Sci U S A 115 (2018) 10678-10683. 10.1073/pnas.1807543115.

[12] N. Yamaguchi, T. Mizutani, K. Kawabata, H. Haga, Leader cells regulate collective cell migration via Rac activation in the downstream signaling of integrin beta1 and PI3K, Sci Rep 5 (2015) 7656. 10.1038/srep07656.

[13] J. Nio, H. Takahashi-Iwanaga, M. Morimatsu, Y. Kon, T. Iwanaga, Immunohistochemical and in situ hybridization analysis of galectin-3, a beta-galactoside binding lectin, in the urinary system of adult mice, Histochem Cell Biol 126 (2006) 45-56. 10.1007/s00418-005-0142-5.

[14] J.Y. Tinevez, N. Perry, J. Schindelin, G.M. Hoopes, G.D. Reynolds, E. Laplantine, S.Y. Bednarek, S.L. Shorte, K.W. Eliceiri, TrackMate: An open and extensible platform for single-particle tracking, Methods 115 (2017) 80-90. 10.1016/j.ymeth.2016.09.016.

[15] S. Ishihara, T. Mizutani, K. Kawabata, H. Haga, An improved method for western blotting when extracting proteins from mammalian cells cultured on a collagen gel under serum-free conditions, Cytotechnology 68 (2016) 25-32. 10.1007/s10616-014-9766-4.

[16] X. Li, S. Ishihara, M. Yasuda, T. Nishioka, T. Mizutani, M. Ishikawa, K. Kawabata, H. Shirato, H. Haga, Lung cancer cells that survive ionizing radiation show increased integrin alpha2beta1- and EGFR-dependent invasiveness, PLoS One 8 (2013) e70905. 10.1371/journal.pone.0070905.

[17] M.L. Nystrom, G.J. Thomas, M. Stone, I.C. Mackenzie, I.R. Hart, J.F. Marshall, Development of a quantitative method to analyse tumour cell invasion in organotypic culture, J Pathol 205 (2005) 468-475. 10.1002/path.1716.

[18] W. Nishie, D. Kiritsi, A. Nystrom, S.C. Hofmann, L. Bruckner-Tuderman, Dynamic interactions of epidermal collagen XVII with the extracellular matrix: laminin 332 as a major binding partner, Am J Pathol 179 (2011) 829-837. 10.1016/j.ajpath.2011.04.019.

[19] K. Tasanen, J.A. Eble, M. Aumailley, H. Schumann, J. Baetge, H. Tu, P. Bruckner, L. Bruckner-Tuderman, Collagen XVII is destabilized by a glycine substitution mutation in the cell adhesion domain Col15, J Biol Chem 275 (2000) 3093-3099.

[20] F. Decline, P. Rousselle, Keratinocyte migration requires alpha2beta1 integrin-mediated interaction with the laminin 5 gamma2 chain, J Cell Sci 114 (2001) 811-823.

[21] F.G. Giancotti, E. Ruoslahti, Integrin signaling, Science 285 (1999) 1028-1032.

[22] J.D. Whittard, S.K. Akiyama, Activation of beta1 integrins induces cell-cell adhesion, Exp Cell Res 263 (2001) 65-76. 10.1006/excr.2000.5099.

[23] E. Serres, F. Debarbieux, F. Stanchi, L. Maggiorella, D. Grall, L. Turchi, F. Burel-Vandenbos, D. Figarella-Branger, T. Virolle, G. Rougon, E. Van Obberghen-Schilling, Fibronectin expression in glioblastomas promotes cell cohesion, collective invasion of basement membrane in vitro and orthotopic tumor growth in mice, Oncogene 33 (2014) 3451-3462. 10.1038/onc.2013.305.

[24] M. Durbeej, Laminins, Cell Tissue Res 339 (2010) 259-268. 10.1007/s00441-009-0838-2.

[25] N. Zahir, J.N. Lakins, A. Russell, W. Ming, C. Chatterjee, G.I. Rozenberg, M.P.

Marinkovich, V.M. Weaver, Autocrine laminin-5 ligates alpha6beta4 integrin and activates RAC and NFkappaB to mediate anchorage-independent survival of mammary tumors, J Cell Biol 163 (2003) 1397-1407. 10.1083/jcb.200302023.

[26] M. Nishimura, W. Nishie, Y. Shirafuji, S. Shinkuma, K. Natsuga, H. Nakamura, D. Sawamura, K. Iwatsuki, H. Shimizu, Extracellular cleavage of collagen XVII is essential for correct cutaneous basement membrane formation, Hum Mol Genet 25 (2016) 328-339. 10.1093/hmg/ddv478.

Figure Legends

Figure 1.

(A) Illustration of the collagen overlay conditions. (B) Time-lapse observations in the bright field. The arrow indicates the direction of movement of the cells. Bar = 100 μm.

Figure 2.

(A) Immunofluorescent staining of integrin-β1 and F-actin. XY-, YZ-, and ZX-sectional views are shown. Green: Integrin-β1. Red: F-actin. Bar = 25 μm. (B) Immunoelectron microscopy of integrin-β1. Black particles show localization of integrin-β1. The left panel shows the low magnification image. The square area is enlarged in the right panel. The arrow indicates the adherens junction. Bars = 1.4 μm (left) and 300 nm (right). (C) Time-lapse observation in the presence of integrin-β1 inhibitory antibody. The upper panels show treatment with negative control IgG. The lower panels show treatment with the integrin-β1 inhibitory antibody (AIIB2). Concentrations of each antibody are 2.0 μg/mL. Bars = 100 μm. (D) Evaluating method of contact following. A: a cell to be analyzed. B: a cell within 100 μm diameter of A. C: a cell outside of 100 μm diameter of A. (E) Time-lapse observation of A431-H2B cells in the presence of integrin-β1 inhibitory antibody. The upper panels show treatment with negative control IgG. The lower panels show treatment with the integrin-β1 inhibitory antibody. Concentrations of each antibody are 2.0 μg/mL. Bars = 50 μm. (F) Quantification of cosine values, cosθ. Boxplot shows median levels of cosθ under each condition. Boxes show IGR. Bars show maximum and

minimum values within 1.5 IQR. **P<0.01 by Wilcoxon rank sum test (n>49).

Figure 3.

Immunofluorescent staining of ECM proteins and F-actin. (A) COL17 (B) laminin-α3 (C) laminin-β3 XY-, YZ-, and ZX-sectional views are shown. Green: ECM proteins. Red: F-actin. Bars = 25 μm. (D) Time-lapse observation of A431-H2B cells in each knockdown condition. The top panels show the cells treated with negative control siRNA (siNC). Other panels show the cells treated with siRNA targeting COL17A1 (siCOL17A1; second), LAMA3 (siLAMA3: third), LAMB3 (siLAMB3; bottom). Bars = 50 μm. (E) Quantification of cosine values, cosθ. Boxplot shows median levels of cosθ in each condition. Boxes show IGR. Bars show maximum and minimum values within 1.5 IQR. **P<0.01 by Wilcoxon rank sum test (n>40).

Figure 4.

(A, B) Input obtained from A431 cells were immunoprecipitated with anti-COL17 antibody followed by western blotting with indicated antibodies. (C) Representative western blotting. The arrows indicate COL17A1 bands around 180, 120, and 97 kDa. (D) Quantification of (C). The bars represent mean ± SEM. in 3 independent experiments. *P<0.05 by Welch's t-test.

Supplementary Material

Supplementary Figure 1.

(A) Time-lapse observation of A431-H2B cells in the fluorescent field. The arrow indicates the direction movement of the cells. Bar = 100 μm. (B) Immunofluorescent staining of active integrin-β1 and F-actin. XY-, YZ-, and ZX-sectional views are shown. Green: Active integrin-β1. Red: F-actin. Bar = 25 μm. (C) Western blotting for detection of COL17 with whole cell lysate derived from siNC cells and siCOL17A1 cells. The graph shows the quantification of band intensity. (D) The graph shows the results of quantitative PCR with cDNA of siNC cells and siLAMA3 cells. The bars represent mean ± SEM. (n=3). (E) Western blotting for detection of LAMB3 with whole cell lysate derived from siNC cells and siLAMB3 cells. The graph shows the quantification of band intensity.

Supplementary Figure 2.

(A) Immunofluorescent staining of phosphorylated FAK Tyr397 (pFAK397) and F-actin. XY-, YZ-, and ZX-sectional views are shown. Green: pFAK397. Red: F-actin. Bar = 25 μm. (B) Immunofluorescent staining of pFAK397 and F-actin 24 hours after AIIB2 treatment. The images of maximum intensity projection are shown. Green: pFAK397. Red: F-actin. Bar = 25 μm.

Figure 1

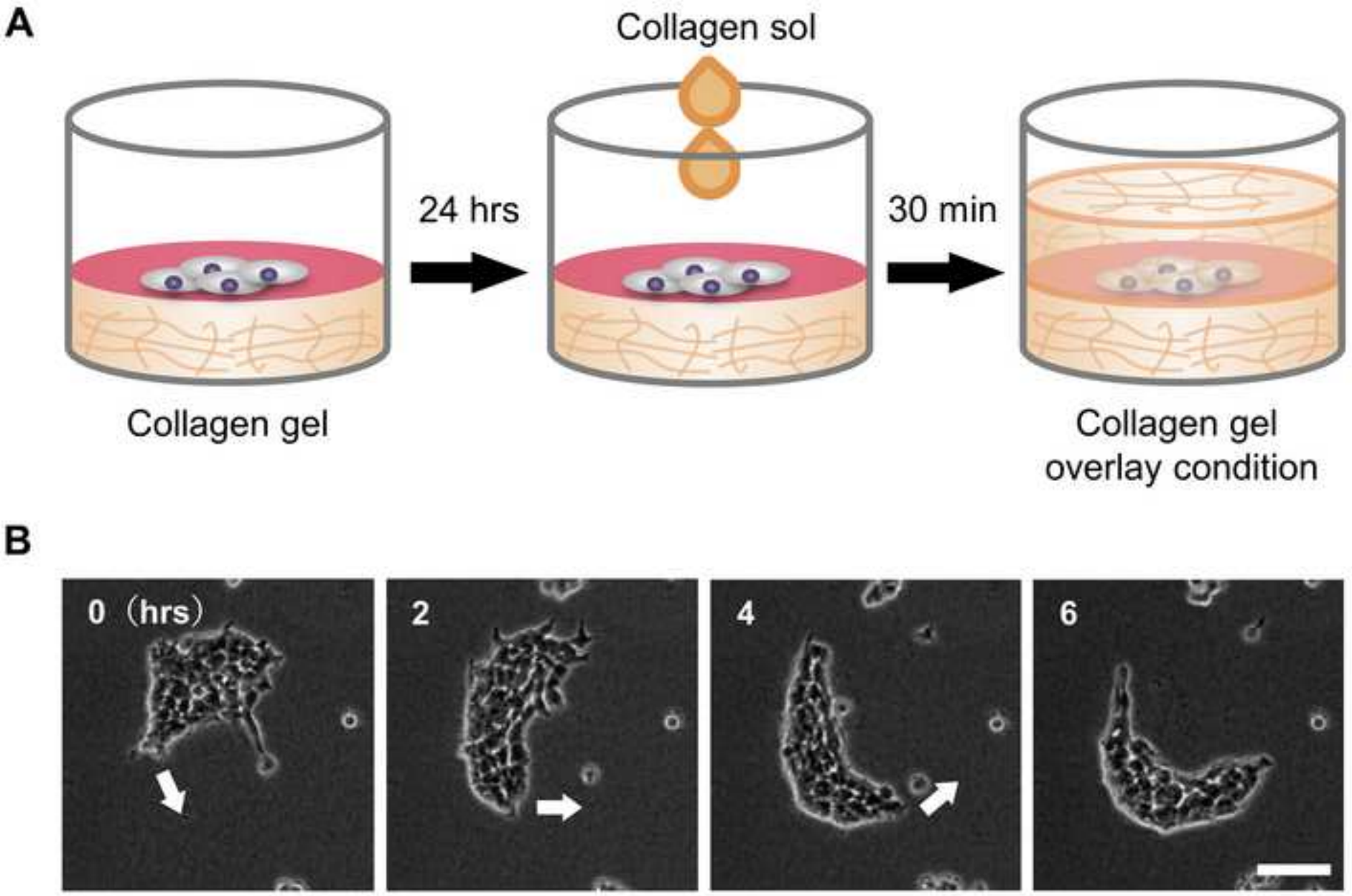
A
Collagen sol
24 hrs
30 min
Collagen gel
Collagen gel
overlay condition
B
0 (hrs)
2
4
6

Figure 2

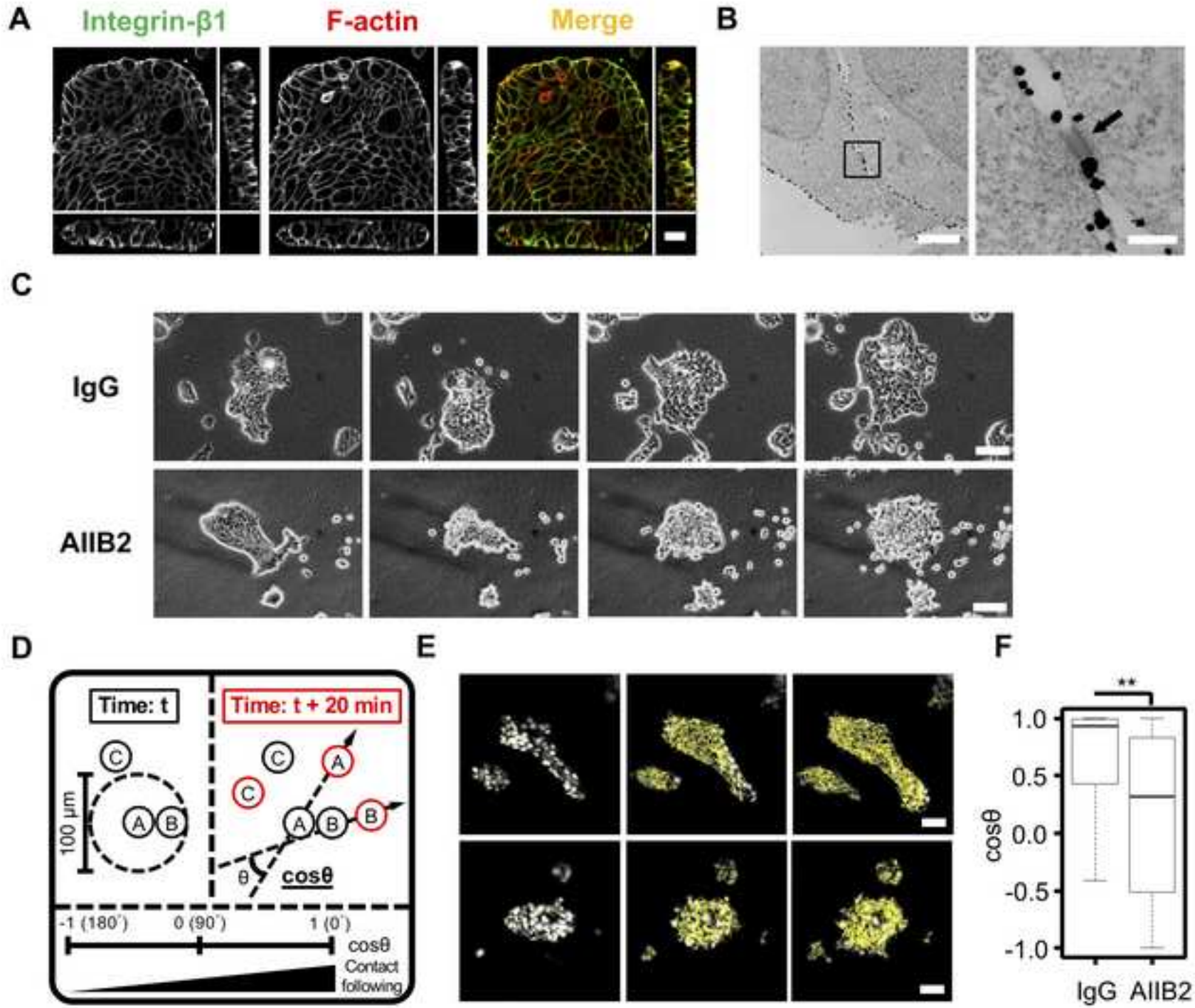
A
Integrin-β1
F-actin
Merge
B
C
IgG
AIIB2
D
Time: t
Time: t + 20 min
100 μm
A
B
C
θ
cosθ
-1 (180°)
0 (90°)
1 (0°)
cosθ
Contact following
E
F
**
1.0
0.5
0.0
-0.5
-1.0
cosθ
IgG
AIIB2

Figure 3

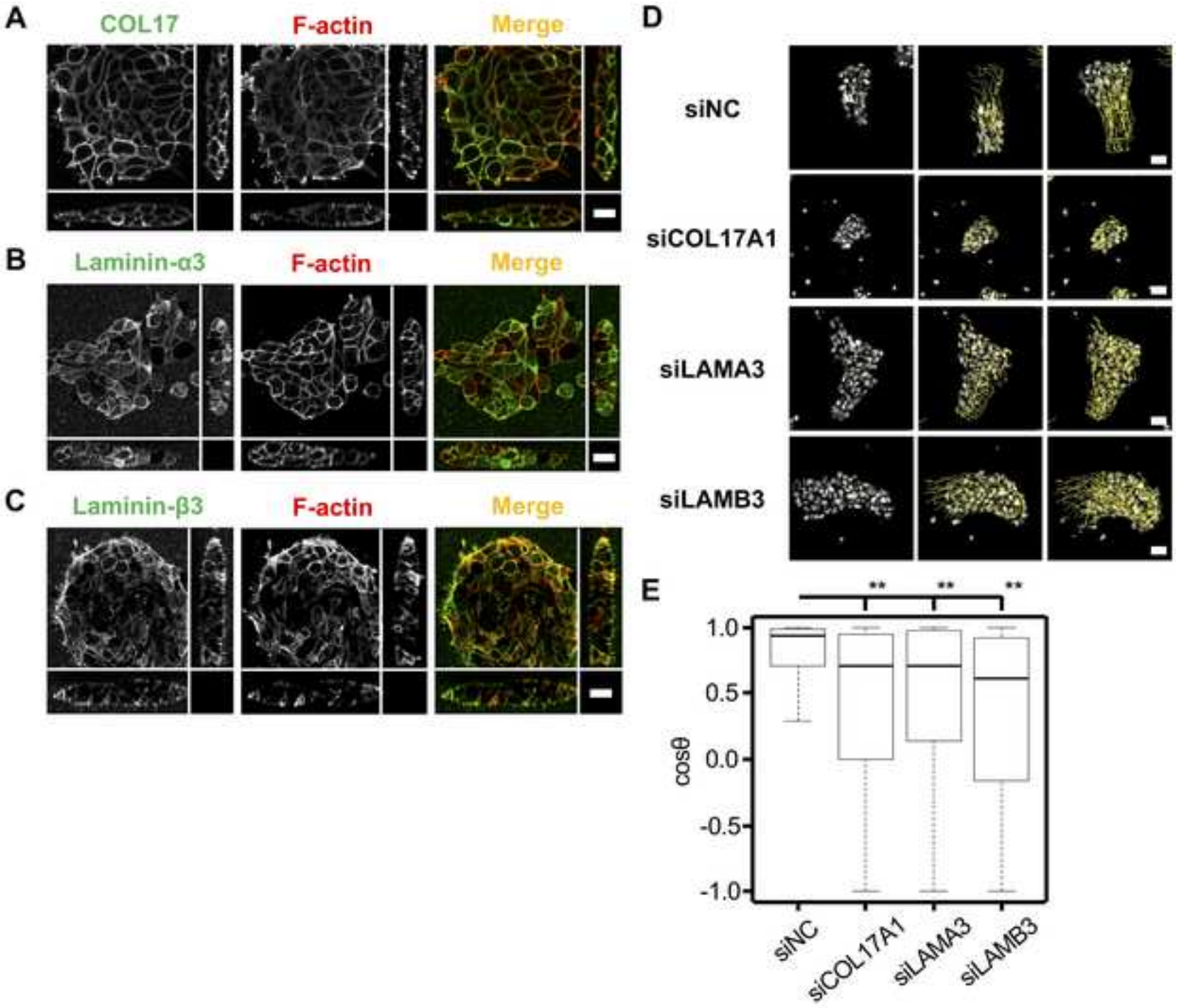
A
COL17
F-actin
Merge
B
Laminin-α3
F-actin
Merge
C
Laminin-β3
F-actin
Merge
D
siNC
siCOL17A1
siLAMA3
siLAMB3
E
**
**
**
1.0
0.5
0.0
-0.5
-1.0
cosθ
siNC
siCOL17A1
siLAMA3
siLAMB3

Figure 4

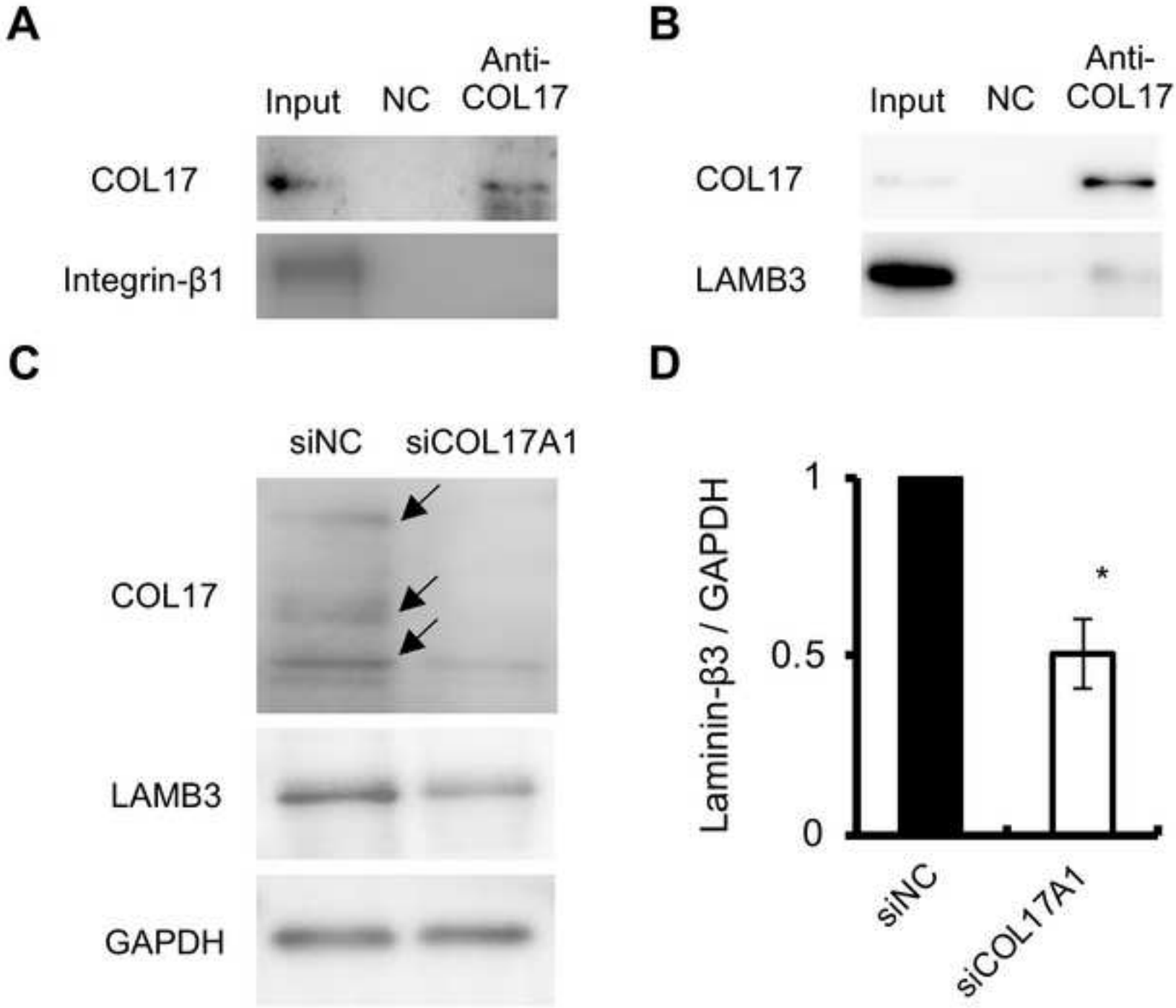
A
Input
NC
Anti-COL17
COL17
Integrin-β1
B
Input
NC
Anti-COL17
COL17
LAMB3
C
siNC
siCOL17A1
COL17
LAMB3
GAPDH
D
Laminin-β3 / GAPDH
1
0.5
0
*
siNC
siCOL17A1

Supplementary Fig. 1

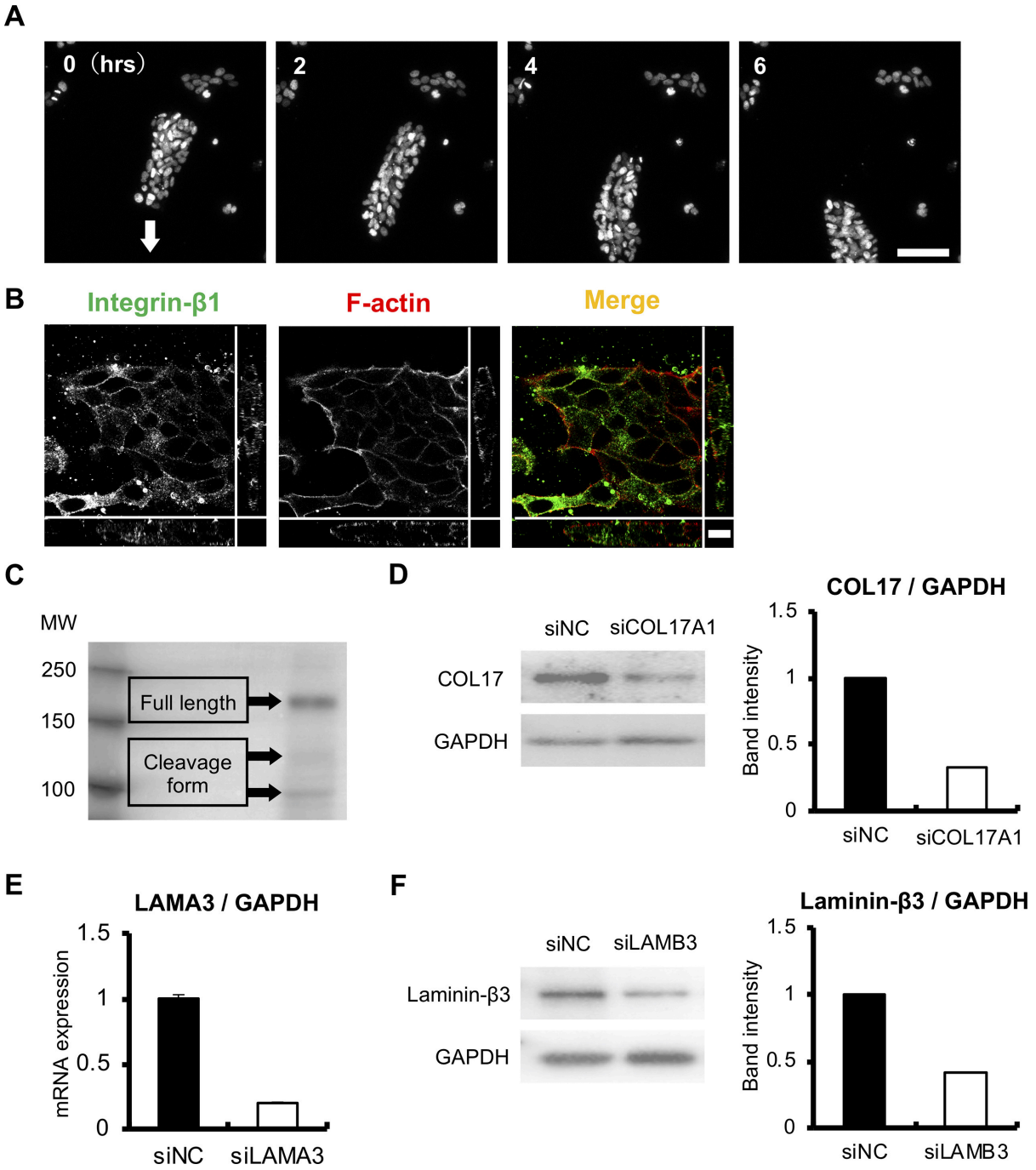

Supplementary Fig. 2